Research Article

Decorin knockdown is beneficial for aged tendons in the presence of biglycan expression

Zakary M. Beach [a], Mihir S. Dekhne [a], Ashley B. Rodriguez [a], Stephanie N. Weiss [a], Thomas H. Adams [b], Sheila M. Adams [b], Mei Sun [b], David E. Birk [b] and Louis J. Soslowsky [a]*

a* - *McKay Orthopaedic Research Laboratory, *University of Pennsylvania, Stemmler Hall, 36th and Hamilton Walk, Philadelphia, PA 19104-6081, United States*

b* - *Department of Molecular Pharmacology & Physiology, *Morsani College of Medicine, University of South Florida, Tampa, FL 33612, United States*

Correspondence to Louis J. Soslowsky: McKay Orthopaedic Research Laboratory, 307A Stemmler Hall, 3450 Hamilton Walk, Philadelphia, PA 19104-6081, United States. *soslowsk@upenn.edu (L.J. Soslowsky)*
https://doi.org/10.1016/j.mbplus.2022.100114

Abstract

Decorin and biglycan are two major small leucine-rich proteoglycans (SLRPs) present in the tendon extracellular matrix that facilitate collagen fibrillogenesis, tissue turnover, and cell signal transduction. Previously, we demonstrated that knockout of decorin prevented the decline of tendon mechanical properties that are associated with aging. The objective of this study was to determine the effects of decorin and biglycan knockdown on tendon structure and mechanics in aged tendons using tamoxifen-inducible knockdown models. We hypothesized that the knockdown of decorin and compound knockdown of decorin and biglycan would prevent age-related declines in tendon mechanics and structure compared to biglycan knockdown and wild-type controls, and that these changes would be exacerbated as the tendons progress towards geriatric ages. To achieve this objective, we created tamoxifen-inducible mouse knockdown models to target decorin and biglycan gene inactivation without the abnormal tendon development associated with traditional knockout models. Knockdown of decorin led to increased midsubstance modulus and decreased stress relaxation in aged tendons. However, these changes were not sustained in the geriatric tendons. Knockdown in biglycan led to no changes in mechanics in the aged or geriatric tendons. Contrary to our hypothesis, the compound decorin/biglycan knockdown tendons did not resemble the decorin knockdown tendons, but resulted in increased viscoelastic properties in the aged and geriatric tendons. Structurally, knockdown of SLRPs, except for the 570d I-*Dcn*$^{-/-}$/*Bgn*$^{-/-}$ group, resulted in alterations to the collagen fibril diameter relative to wild-type controls. Overall, this study identified the differential roles of decorin and biglycan throughout tendon aging in the maintenance of tendon structural and mechanical properties and revealed that the compound decorin and biglycan knockdown phenotype did not resemble the single gene decorin or biglycan models and was detrimental to tendon properties throughout aging.

© 2022 The Author(s). Published by Elsevier B.V. This is an open access article under the CC BY-NC-ND license (http://creativecommons.org/licenses/by-nc-nd/4.0/).

0022-2836/© 2022 The Author(s). Published by Elsevier B.V.This is an open access article under the CC BY-NC-ND license (http://creativecommons.org/licenses/by-nc-nd/4.0/).

Introduction

Tendon is a hierarchically organized tissue composed of highly aligned extracellular matrix (ECM) whose predominant function is to transmit tensile forces from muscle to bone. The primary unit of the tendon is the tendon fibril, a heteropolymeric structure assembled from multiple fibril-forming collagens, glycoproteins, glycosaminoglycans (GAGs), and proteoglycans [1]. A major component of proteoglycans in tendon are small leucine-rich proteoglycans (SLRPs), which are a class of proteins involved in a variety of biological processes including collagen fibrillogenesis, tissue turnover, and cell signal transduction [2]. Decorin (Dcn) and biglycan (Bgn) are two highly expressed fibril associated class I SLRPs that assist in the development and maintenance of tendon structure during development, homeostasis, healing, and aging by binding fibrillar collagens and regulating fibrillogenesis [3–8]. Fibromodulin, lumican, and keratocan are class II SLRPs that are structurally and functionally similar to decorin and biglycan, and regulate fibrillogenesis by binding to fibrillar collagens. Gene clustering balances the expression of these SLRPs, creating a regulatory network among these molecules. This regulatory network can result in compensatory upregulation of other SLRPs after knockdown of one of these genes. Due to the functional redundancy between fibril associated SLRPs during fibrillogenesis, it is important to investigate the expression of all these molecules when using knockdown models to better understand these relationships. Given the wide range of processes in which these proteins are involved, a complete definition of their individual and synergistic roles is required for developing novel treatments to address tendon pathologies.

With an increasingly aging and active population the incidence of tendon injury is on the rise [9]. Tendon aging is typically characterized by changes to mechanics and structure including decreased stiffness, modulus, and alterations to collagen fibril diameter [7,10]. While the mechanisms that cause tissue to become more susceptible to injury with increased age are largely unknown, SLRPs are known regulators of collagen fibril organization and matrix assembly in tendon, and could play a role in the age-related changes to tendon mechanics and structure. Previous work using traditional (non-inducible) mouse knockout models found that knockout of decorin ameliorated the age-related alterations to mechanics and structure that is normally observed in tendon, while minimal changes were associated with knockout of biglycan [7]. The traditional knockout models used previously found upregulation of lumican after biglycan knockout, potentially masking the true roles of biglycan during aging, and did not allow for temporal control of SLRP expression.

While studies have been conducted to explore the roles of decorin and biglycan in tendon aging, these results are confounded due to the limitations inherent to traditional knockouts that cannot isolate effects during aging from developmental effects. Recently, our lab has utilized tamoxifen-inducible decorin, biglycan, and compound decorin and biglycan knockdown mouse models to provide temporal control over SLRP expression. The compound model was initially used to determine the roles of decorin and biglycan during tendon homeostasis in mature mice 30 days after Cre induction. Despite the short timeline, the model successfully resulted in reduced decorin and biglycan gene and protein expression levels as well as a decrease in mechanical and structural properties of the mouse patellar tendon [11]. The present study extends this work by utilizing tamoxifen-inducible decorin, biglycan, and the compound decorin and biglycan knockdown models to study the effects of these proteins on tendon structure and function in aged tendons without disrupting tendon development.

Therefore, the objective of this study was to determine the effects of decorin and biglycan knockdown on tendon structure and mechanics in aged (300d) and geriatric (570d) tendons. We hypothesized that decorin and compound decorin/biglycan knockdown in aged and geriatric mice would result in improved tendon mechanical properties compared to biglycan knockdown and wild type (WT) control mice. We also expected to find alterations to tendon fibril structure after decorin or biglycan knockdown, while the compound decorin/biglycan knockdown mice were expected to have a fibril phenotype identical to the decorin knockdown mice. Further, we hypothesized that the differences present in the aged tendons would be exacerbated in the geriatric tendons. Overall, our findings revealed that knockdown of decorin attenuates the decline in tendon mechanics associated with aging in aged (but not geriatric) mice, and knockdown of decorin and biglycan produced tendons with increased viscoelastic mechanics with age.

Results

Isolated knockdown of decorin and biglycan did not induce upregulation of other fibril-associated SLRPs

The expression of various SLRPs were analyzed to investigate compensatory upregulation within our transgenic models. Expression levels confirmed knockdown of decorin and biglycan in the respective transgenic models at 300d and 570d, and no compensation was present among the class I SLRPs in the single-target models (Fig. 1A-B, D-E). To confirm that the transgenic models did

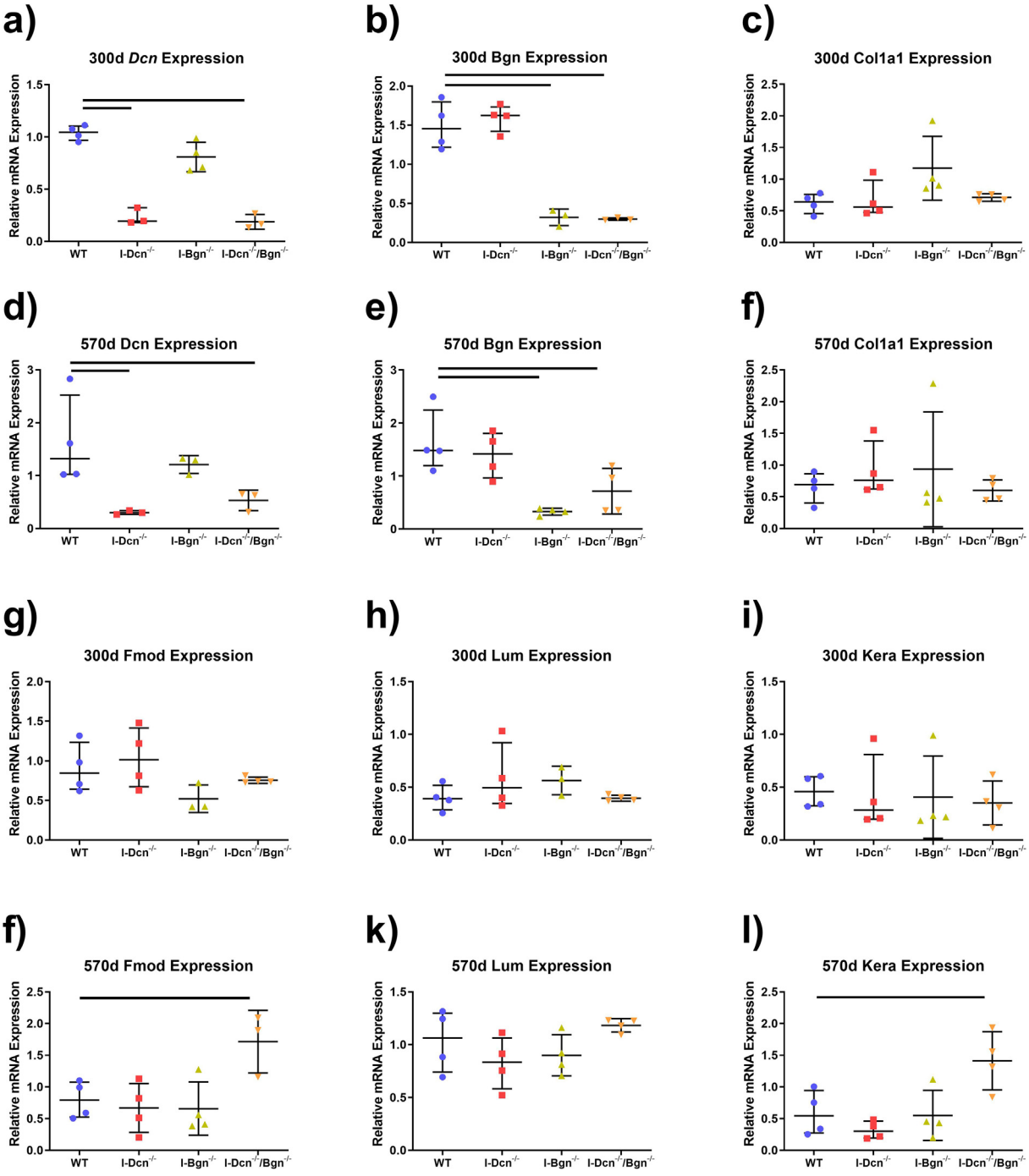

Fig. 1. SLRP and Collagen I Gene Expression in Aged and Geriatric Mouse Patellar Tendons. Gene expression was measured at 300 d and 570 d after Cre induction at 120 d (n = 3-4/genotype/age). Knockdown of *Dcn* was confirmed in I-*Dcn*$^{-/-}$ and I-*Dcn*$^{-/-}$/*Bgn*$^{-/-}$ tendons (a, d) and knockdown of Bgn was confirmed for I-*Bgn*$^{-/-}$ and I-*Dcn*$^{-/-}$/*Bgn*$^{-/-}$ tendons (b, e) at 370d and 570d. No upregulation of *Dcn* or *Bgn* was detected in I-*Dcn*$^{-/-}$ or I-*Bgn*$^{-/-}$ tendons, respectively, at 300 d or 570 d (a, b, d, e). No changes in *Col1a1* were detected between genotypes at 300 d or 570 d (c, f). Increased compensatory expression of *Fmod* (j) and *Kera* (l) was detected in I-*Dcn*$^{-/-}$/*Bgn*$^{-/-}$ tendons. Data shown as median with interquartile range.

not alter expression of collagen I *Col1a1* expression was measured, and no changes in expression were found at either timepoint (Fig. 1C, F). Finally, to determine if compensation was present among the class II SLRPs, we measured fibromodulin, lumican, and keratocan expression. No compensation of class II SLRPs was observed within any of the transgenic models at 300d

(Fig. 1G-I). The lack of class II SLRP compensation was constant for the I-*Dcn*$^{-/-}$ and I-*Bgn*$^{-/-}$ models at 570d (Fig. 1J-L). Fibromodulin (Fig. 1J) and keratocan (Fig. 1L) were upregulated in I-*Dcn*$^{-/-}$/*Bgn*$^{-/-}$ tendons at 570d, while lumican (Fig. 1K) was not. Overall, each of the transgenic models demonstrated effective knockdown of the target genes, and no compensation of SLRPs was present in the I-*Dcn*$^{-/-}$ or I-*Bgn*$^{-/-}$ models. The compound knockdown of decorin and biglycan was compensated with increased fibromodulin and keratocan expression at 570d.

Decorin and biglycan knockdown increased viscoelastic mechanics with age while decorin knockdown attenuated Age-Related decline in mechanics

After determining that minimal masking effects were present from upregulation of SLRPs in our knockdown models we determined the effects of decorin and biglycan knockdown on tendon mechanics. Before sacrifice no changes in gait were noted among the mice. I-*Dcn*$^{-/-}$ tendons had an increased midsubstance modulus at 300d (Fig. 2A) compared to WT and I-*Dcn*$^{-/-}$/*Bgn*$^{-/-}$. Decorin knockdown did not produce the same increase in midsubstance modulus at 570d, where no changes across the genotypes were observed (Fig. 2B). Additionally, no changes in the insertion modulus were found at 300d or 570d (Fig. 2C, D). Stress-relaxation tests performed at 3 % strain found decreased relaxation in I-*Dcn*$^{-/-}$ tendons compared to WT and I-*Dcn*$^{-/-}$/*Bgn*$^{-/-}$ at 300d (Fig. 2E), and I-*Dcn*$^{-/-}$/*Bgn*$^{-/-}$ had increased relaxation compared to WT at 570d (Fig. 2F). Additionally, relaxation increased between 300d and 570d for I-*Dcn*$^{-/-}$ tendons (Fig. 2E, F). However, there was a significant interaction between genotype and age during the stress-relaxation tests performed at 3 % strain. At 4 % strain I-*Dcn*$^{-/-}$/*Bgn*$^{-/-}$ showed increased relaxation compared to I-*Dcn*$^{-/-}$ at 300d (Fig. 2G) and increased relaxation compared to WT, I-*Dcn*$^{-/-}$, and I-*Bgn*$^{-/-}$ at 570d (Fig. 2H). Stress relaxation at 5 % strain did not change between groups (Fig. 2I, J).

To further determine the roles of decorin and biglycan in aging tendon viscoelastic mechanics we measured the dynamic modulus (E*) and phase shift (tangent of loss angle, tan (δ)) during dynamic loading. E* and phase shift showed no changes between genotypes at 300d or 570d, but changes were found within genotypes between ages. Specifically, I-*Dcn*$^{-/-}$ reduced dynamic modulus at 3 % and 4 % strain across all loading frequencies, and at 5 % strain at 0.1 and 1 Hz (Fig. 3A). Changes in phase angle shift were also found between 300d and 570d for both I-*Dcn*$^{-/-}$ (Fig. 3B) and I-*Dcn*$^{-/-}$/*Bgn*$^{-/-}$ (Fig. 3C) tendons. Reductions in I-*Dcn*$^{-/-}$ phase shift were observed at 3 % strain at 1, 5, and 10 Hz, 4 % strain at 0.1, 1, 5, and 10 Hz, and 5 % strain at 0.1, 5, and 5 Hz. I-*Dcn*$^{-/-}$/Bgn$^{-/-}$ reductions in phase shift were found at 3 % strain at 0.1, 1, and 5 Hz and 4 % strain at 5 Hz.

Small Leucine-rich proteoglycan knockdown produced minimal changes to collagen fiber realignment

Decreased circular variance ratio, which correlates with increased collagen fiber realignment, was found for WT and I-*Dcn*$^{-/-}$ tendons at 300d (Fig. 4A) and I-*Dcn*$^{-/-}$/*Bgn*$^{-/-}$ tendons at 570d between 1 % and 3 % strain (Fig. 4B). Analysis of the midsubstance revealed increased realignment for WT, I-*Dcn*$^{-/-}$, I-*Bgn*$^{-/-}$, and I-*Dcn*$^{-/-}$/*Bgn*$^{-/-}$ tendons at 300d (Fig. 4C) and 570d (Fig. 4D) between 1 % and 3 % strain, and no further realignment occurred at 5 % or 7 % strain. No differences in realignment were found in either the insertion or midsubstance between genotypes or ages.

Alterations to collagen fibril diameter were consistently present after knockdown of decorin and biglycan

After TEM imaging no gross changes to fibril shape were apparent after SLRP knockdown in aged or geriatric tendon (Fig. 5A). 300d I-*Dcn*$^{-/-}$, I-*Bgn*$^{-/-}$, and I-*Dcn*$^{-/-}$/*Bgn*$^{-/-}$ tendons revealed altered fibril diameter distributions compared to WT tendons (Fig. 5B, C). Additionally, at 300d, the I-*Dcn*$^{-/-}$ tendon collagen fibrils showed increased diameter heterogeneity and decreased minimum fibril diameter. At 570d only I-*Dcn*$^{-/-}$ and I-*Bgn*$^{-/-}$ tendons exhibited altered collagen fibril diameter distributions compared to WT. The I-*Dcn*$^{-/-}$ tendons also displayed reduced fibril diameter in quartiles 2–4 of the fibril diameter distribution compared to WT (Fig. 5B, D).

Biglycan knockdown resulted in minimal changes to nuclear shape in aged tendons

Tendons were stained with hematoxylin and eosin to visualize the macroscopic tendon structure and cellular population to measure cellularity and nuclear aspect ratio. No abnormalities were present in the overall tendon structure at 300d or 570d (Fig. 6A, B). Cells present in the I-*Bgn*$^{-/-}$ tendons exhibited an increased nuclear aspect ratio, indicating a more rounded nuclear shape, compared to WT and I-*Dcn*$^{-/-}$/*Bgn*$^{-/-}$ tendon cells at the 300d timepoint (Fig. 6C), while no changes were present between the genotypes at 570d (Fig. 6D). No changes were found in cellularity between genotypes at 300d or 570d (data not shown).

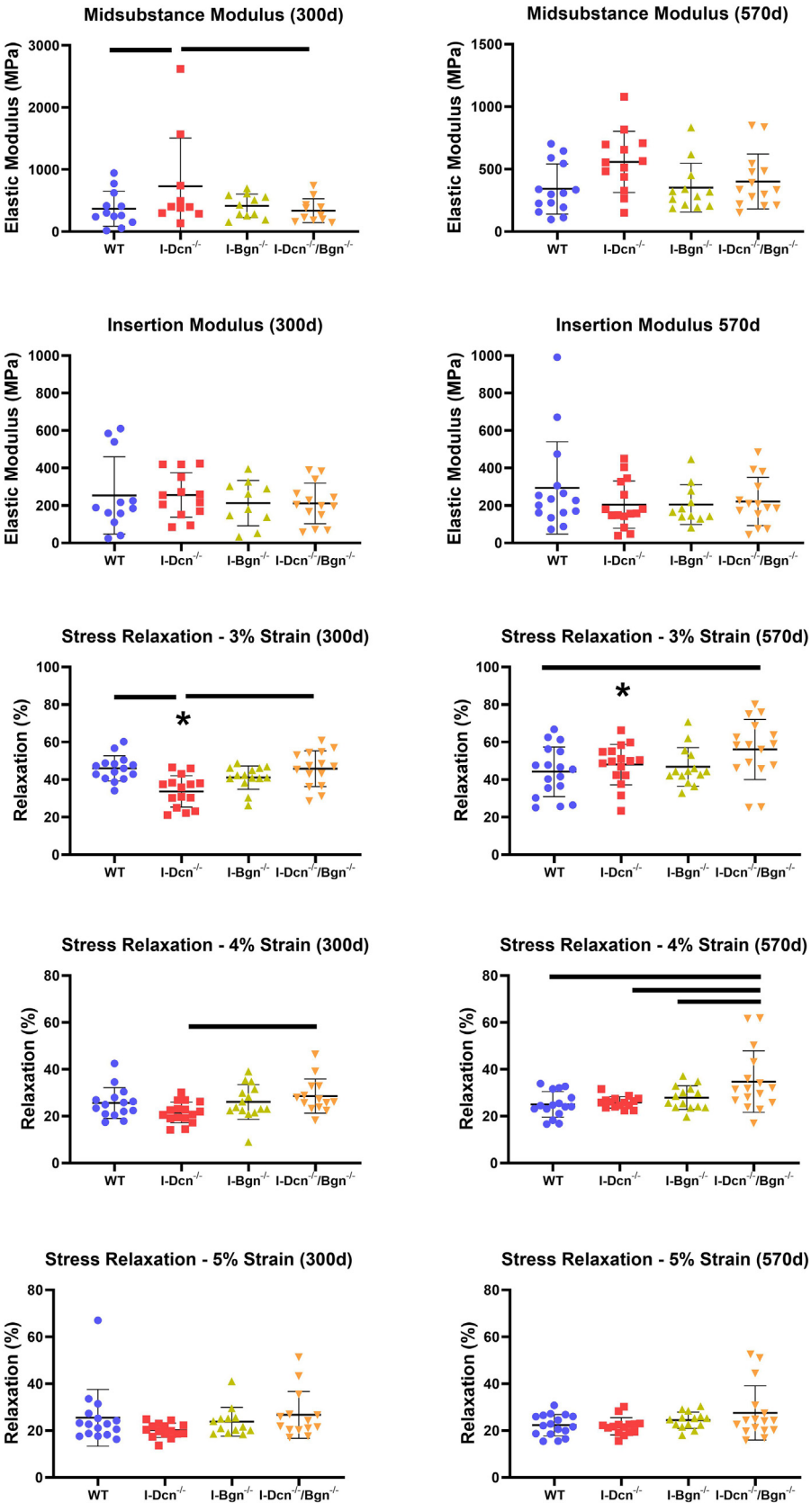
Midsubstance Modulus (300d)
Elastic Modulus (MPa)
3000
2000
1000
0
WT
I-Dcn-/-
I-Bgn-/-
I-Dcn-/-/Bgn-/-
Midsubstance Modulus (570d)
Elastic Modulus (MPa)
1500
1000
500
0
WT
I-Dcn-/-
I-Bgn-/-
I-Dcn-/-/Bgn-/-
Insertion Modulus (300d)
Elastic Modulus (MPa)
1000
800
600
400
200
0
WT
I-Dcn-/-
I-Bgn-/-
I-Dcn-/-/Bgn-/-
Insertion Modulus 570d
Elastic Modulus (MPa)
1000
800
600
400
200
0
WT
I-Dcn-/-
I-Bgn-/-
I-Dcn-/-/Bgn-/-
Stress Relaxation - 3% Strain (300d)
Relaxation (%)
100
80
60
40
20
0
*
WT
I-Dcn-/-
I-Bgn-/-
I-Dcn-/-/Bgn-/-
Stress Relaxation - 3% Strain (570d)
Relaxation (%)
100
80
60
40
20
0
*
WT
I-Dcn-/-
I-Bgn-/-
I-Dcn-/-/Bgn-/-
Stress Relaxation - 4% Strain (300d)
Relaxation (%)
80
60
40
20
0
WT
I-Dcn-/-
I-Bgn-/-
I-Dcn-/-/Bgn-/-
Stress Relaxation - 4% Strain (570d)
Relaxation (%)
80
60
40
20
0
WT
I-Dcn-/-
I-Bgn-/-
I-Dcn-/-/Bgn-/-
Stress Relaxation - 5% Strain (300d)
Relaxation (%)
80
60
40
20
0
WT
I-Dcn-/-
I-Bgn-/-
I-Dcn-/-/Bgn-/-
Stress Relaxation - 5% Strain (570d)
Relaxation (%)
80
60
40
20
0
WT
I-Dcn-/-
I-Bgn-/-
I-Dcn-/-/Bgn-/-

Discussion

Though the roles of decorin and biglycan in aged and geriatric tendons have been previously considered, this is the first study to examine the differential and combined roles of decorin and biglycan at these ages in tendon without the confounding effects of abnormal tendon development. This was achieved using TM-inducible SLRP knockdown mouse models that allowed decorin and biglycan knockdown after musculoskeletal maturity. We hypothesized that the knockdown of decorin and compound decorin/biglycan knockdown in aged and geriatric mice would result in improved tendon mechanical properties compared to the biglycan knockdown and WT tendons. Additionally, we expected alterations to the tendon fibril structure after decorin or biglycan knockdown, while the compound decorin/biglycan knockdown tendon fibril structure would resemble the structure of the decorin knockdown tendons. Furthermore, we hypothesized that the changes found in the aged tendons would be exacerbated in the geriatric tendons. A multidisciplinary approach was utilized to determine that decorin and biglycan play important differential roles in the regulation of tendon mechanics and structure during aging. In support of our hypotheses, the knockdown of decorin resulted in an improved tendon aging phenotype while knockdown of biglycan had no impact on mechanics. We also found that the knockdown of decorin or biglycan resulted in alterations to tendon structure. Contrary to our hypothesis, the compound decorin/biglycan knockdown model did not mimic the decorin knockdown model and resulted in increased viscoelastic mechanics with age.

TM-inducible knockdown models were utilized in this study to allow for normal development with the targeted genes activated, avoiding the confounding effects of abnormal development associated with traditional knockout models [12,13]. TM-inducible models require TM treatment for Cre activation and subsequent excision of the target genes. This process occurs after TM metabolizes into 4-hydroxytamoxifen, which binds to an estrogen receptor and enables translocation of the CreERT2 complex into the nucleus [14]. The ability for 4-hydroxytamoxifen to bind to estrogen receptors may interfere with the estrogen pathway and result in unintended side effects during tendon homeostasis [15]. While TM treatment may result in temporary disruption of the estrogen pathway, the long timeline and treatment of control groups with TM in this study mitigates any impact of unintended side effects that TM may cause during tendon homeostasis.

To elucidate the regulatory roles of decorin and biglycan throughout tendon aging two timepoints were used that correlate with aged and geriatric mice. 300-day old mice were selected as the aged group because of the decline in mechanical properties of the tendons compared to mature (150-day) mouse tendons combined with the similarities between the survival curves of mice at this age and 60–65-year-old women, where both survival curves fall below an 85 % survival rate [16,17]. The 60–65-year-old population is still active, less sedentary than older populations, but also represent a population where tendon injuries are common [18]. 570-day old mice were used to represent an extremely aged group (termed geriatric) to further define the effects of SLRP knockdown on geriatric tendon because intermediate timepoints did not show additional age-related declines in tendon mechanics compared to 300d, and later time points were not viable due to low survival rates in our SLRP knockdown models.

The improved tendon aging phenotype associated with decorin knockdown has been previously shown using a traditional mouse knockout model, where knockout of decorin resulted in minor decreases in viscoelastic and quasi-static mechanics with age relative to the changes associated with biglycan knockout and WT tendons [7]. It was speculated that decorin knockout improved tendon aging due to its role in fibrillogenesis, where continued decorin-fibril interactions facilitated lateral growth of mature fibrils, resulting in changes to the tendon ultrastructure and mechanical properties. Overall, these results are supported in the current study, where decorin knockdown during homoeostasis in skeletally mature mice resulted in improved quasi-static and viscoelastic mechanics at 300d, although these improvements were no longer present at the 570d time point. Interestingly, we found that knockdown of decorin resulted in a broadening of the collagen fibril diameter distribution at 300d, where improved mechanics were present, and a decrease in the fibril diameter at 570d, where these improvements were

Fig. 2. Patellar Tendon Modulus and Stress Relaxation After Decorin and Biglycan Knockdown. During mechanical testing, the tendon midsubstance (a, b) and insertion (c, d) modulus was measured for 300 d and 570 d tendons, respectively (n = 10–14/genotype/age). A stress-relaxation test was applied to the tendons at 3% (e, f), 4% (g, h), and 5% (i, j) strain to determine the viscoelastic response of the tendons at 300 d and 570 d (mean ± SD, n = 13–16). Data shown as mean ± standard deviation. Bars indicate significance of $p < 0.05/12$ between genotypes at 300 d or 570 d. * indicates significance of $p < 0.05/12$ between 300 d and 570 d within a genotype. Comparisons were made with two-way ANOVAs based on genotype and age with Bonferroni post-hoc comparisons.

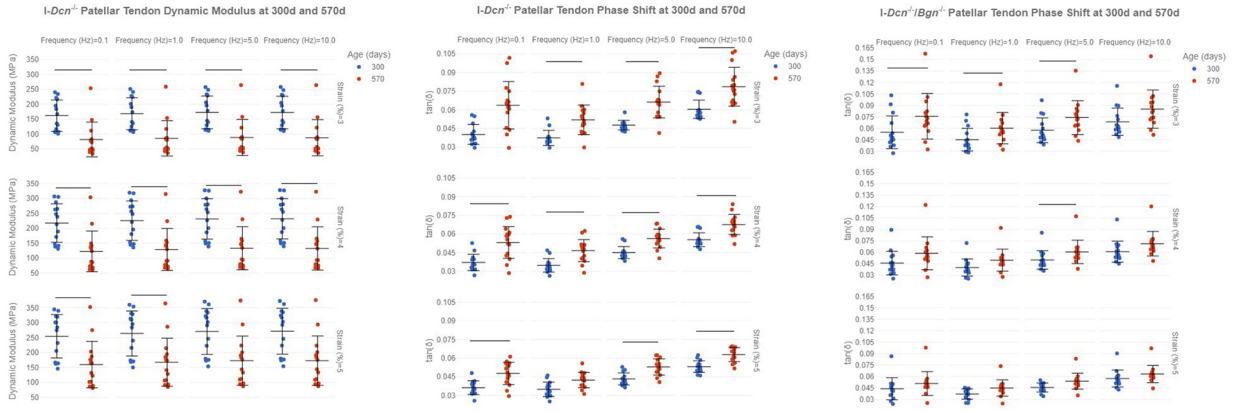

Fig. 3. Age-related Changes to Patellar Tendon Viscoelastic Properties. Tendon viscoelastic properties were evaluated with a series of frequency sweeps at 3%, 4%, and 5% strain at 0.1, 1, 5, and 10 Hz to evaluate the dynamic modulus and phase shift (tangent of the phase angle (δ), n = 10–16/genotype/age). I-*Dcn*$^{-/-}$ tendon viscosity increased with age, represented by decreased elastic modulus (a) and increased phase shift (b). The increased viscous response was less pronounced with age in I-*Dcn*$^{-/-}$/*Bgn*$^{-/-}$ tendons, revealing an increased phase shift at 3% strain while loaded at 0.1, 1, and 5 Hz, and 4% strain at 5 Hz (c). Data shown as mean ± standard deviation. Bars indicate significance of $p<0.05/4$. Comparisons were made with two-way ANOVAs based on genotype and age with Bonferroni post-hoc comparisons. Data for genotypes that did not change with age were not shown.

no longer present. This supports the idea that decorin is a mediator of fibrillogenesis whose role is highly context dependent [19], but a repeatable pattern in how decorin facilitates an improved tendon aging phenotype has not been discovered.

Our dynamic mechanical loading data revealed differences with age within individual genotypes that were not apparent from the quasi-static mechanics. While the quasi-static data did not show differences between 300d and 570d mechanics, dynamic modulus and phase angle shift were sensitive to the changes between 300d and 570d after decorin and compound decorin/biglycan knockdown. This may be due to the proposed role of proteoglycans in maintaining hydrostatic pressure within the tendon by interacting with the fluid phase to support viscoelastic mechanics. However, multiple studies have produced evidence rejecting this hypothesis using various methods to reduce proteoglycan content and deplete the GAG content from SLRPs and the surrounding tissue [20–22]. Alternatively, these differences found may reveal that dynamic loading is more sensitive to changes to tendon structure and function associated with SLRP knockdown since dynamic loading is more representative of the *in vivo* loading environment.

The observation that reduced decorin expression has a greater impact than biglycan expression in tissues rich in collagenous fibers is not new. Previous data suggests that greater impact of decorin deficiency compared to biglycan deficiency on skin integrity is consistent with greater abundance of decorin in the dermis [23]. Additionally, the similarity in ultrastructural changes produced by decorin or biglycan deficiency is consistent with the similar roles that each SLRP plays in interactions with dermal collagen. Similarly, the current study revealed a greater impact from decorin knockdown relative to biglycan knockdown on tendon mechanics; however, the ultrastructural changes to tendon fibril diameter were similar. While the relative abundance of decorin and biglycan likely plays a major role in the effects of knockdown on tendon aging, an additional study examining the effects of decorin and biglycan knockdown during tendon aging noted the roles of biglycan in tendon stem cell regulation. That stem cell regulation will likely have less of an impact during tendon aging due to senescence [24].

Contrary to our hypothesis, the compound knockdown of decorin and biglycan did not mimic the I-Dcn$^{-/-}$ tendons but produced tendons with increased viscoelastic properties. The role of SLRPs in tendon viscoelastic mechanics is controversial. The altered viscoelastic mechanics observed in the 570d I-*Dcn*$^{-/-}$/*Bgn*$^{-/-}$ group cannot be explained by alterations to collagen fibril structure since this group showed no changes in these measures relative to WT. Previous work has suggested that the decorin and biglycan GAG chains play a direct role in the regulation of tendon mechanics [25,26]. However, subsequent studies digested the SLRP GAG chains did not observe any changes to mechanics [21,22,27]. The mechanisms driving the alterations observed in the compound decorin and biglycan knockdown viscoelastic mechanics in our present study are unclear. Knockdown of decorin and biglycan could produce alterations to viscoelastic mechanics due to the wide range of biological functions of these proteins including regulation of various collagens

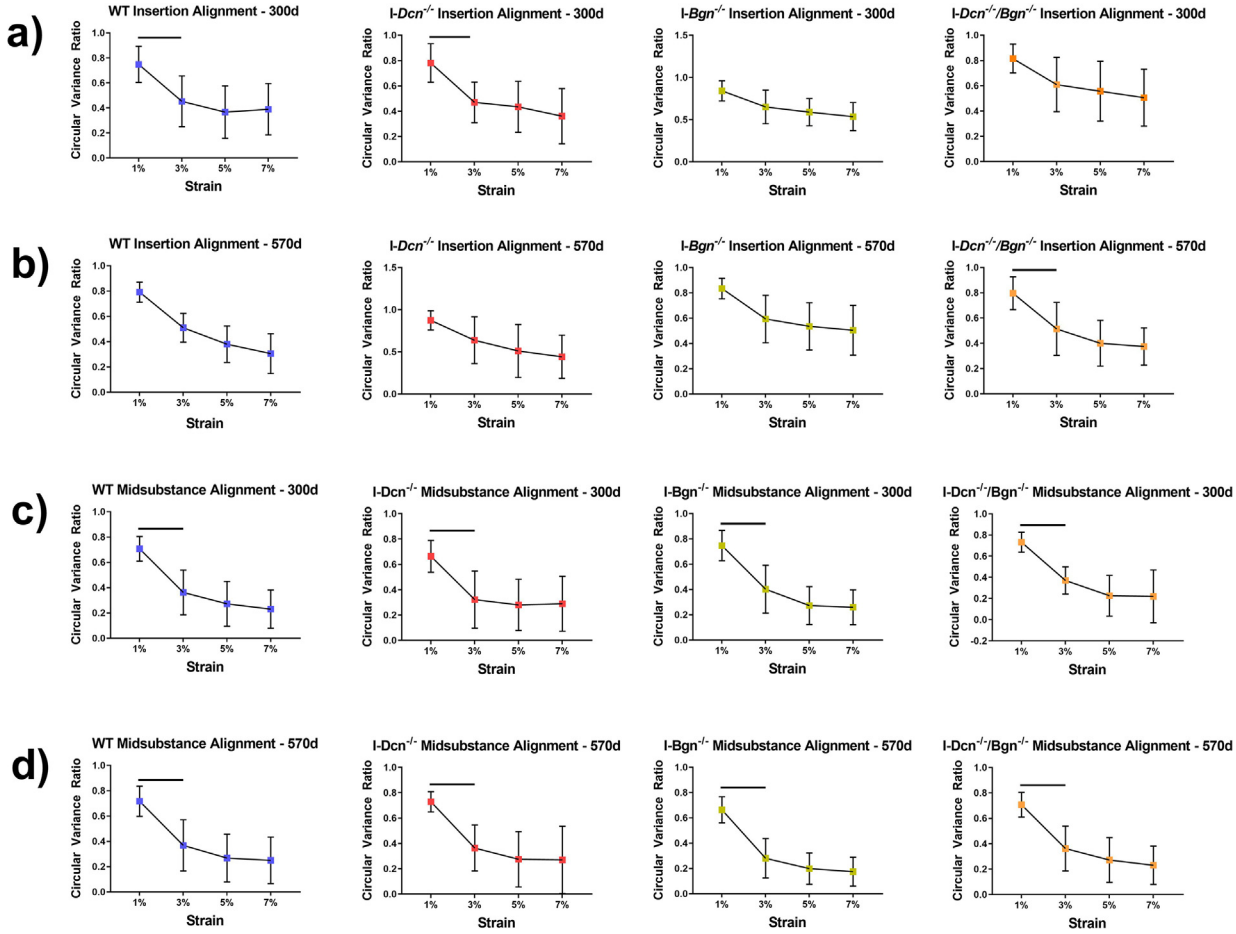

Fig. 4. Collagen Fiber Realignment in the Patellar Tendon Insertion and Midsubstance. Collagen fiber realignment was measured during the ramp to failure by analyzing the circular variance of the collagen fiber distribution angles at 1%, 3%, 5%, and 7% strain, then normalizing those values by the circular variance at 0% strain to obtain the circular variance ratio (n = 10–14/genotype/age). Differential responses were observed in the insertion, with realignment occurring in 300 d WT and I-*Dcn*$^{-/-}$ tendons between 1–3% strain (a), while only I-*Dcn*$^{-/-}$/*Bgn*$^{-/-}$ tendon realignment increased between 1–3% strain at 570 d. All groups demonstrated similar realignment mechanics in the midsubstance, with realignment occurring between 1–3% strain (c, d). Data shown as mean ± standard deviation. Bars indicate significance of $p < 0.05/36$. Comparisons were made with a three-way ANOVA based on genotype, age, and strain with Bonferroni post-hoc comparisons. Strain was the only significant factor.

[19,28–30], innate immune receptors [31], and multiple signaling pathways including TGF-β [32], Wnt [33], and VEGFA [34]. Additionally, the altered viscoelastic properties could be due to the upregulation of class II SLRPs observed at 570d. The upregulation of fibromodulin and keratocan could disrupt additional pathways that are prevalent during tendon aging, such as LOX mediated collagen crosslinking [35–37]. While this study focused on measuring the expression of class I and II fibril-associated SLRPs to determine any compensatory upregulation that may have occurred, a multiomic-based approach can be applied to our I-*Dcn*$^{-/-}$/*Bgn*$^{-/-}$ model at 570d to determine the signaling changes that may be driving the alterations to viscoelastic mechanics.

This study has several limitations. We focused our studies on the patellar tendon, while additional tendons, such as the Achilles, may alter the impact that SLRP knockdown has on tendon mechanics and structure throughout aging. Future work will include additional tendons to broaden the context of our current study. Additionally, this study did not explore functional changes alongside the mechanical and structural analyses. However, our mechanical testing protocol and multi-faceted structural analysis is more sensitive to detecting changes within tendon than functional measurements, such as gait or running analyses. Since no changes in gait were noted among our animals, we chose to not include any of these functional measures. Finally, this study used gene expression to validate knockdown in our models and did not include protein measures. We have previously validated that knockdown of decorin and biglycan

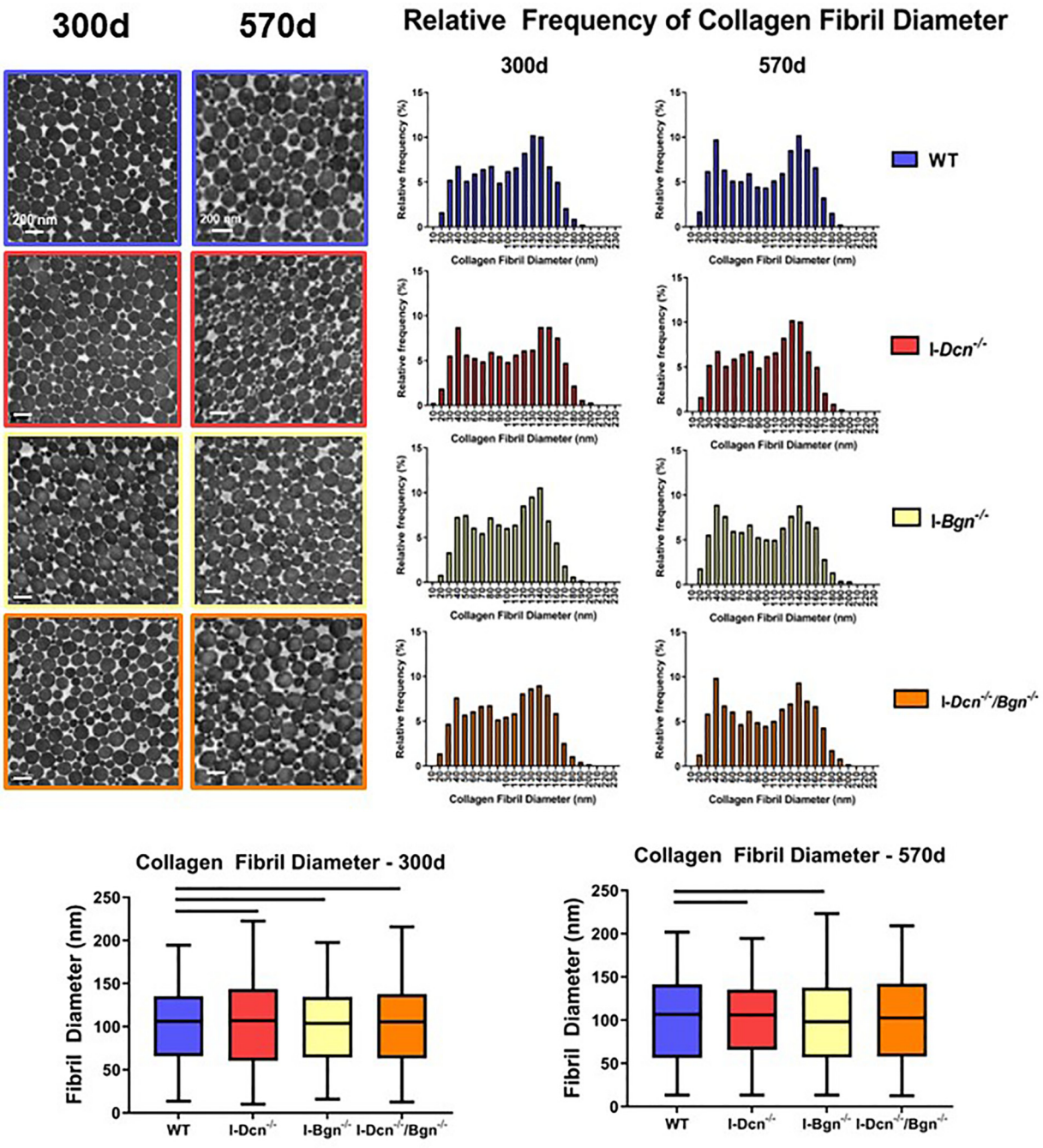

Fig. 5. Effect of Decorin and Biglycan Knockdown on Patellar Tendon Collagen Fibril Diameter. Tendon microstructure was examined using transmission electron microscopy to measure collagen fibril diameter (a, n = 4/genotype/age). After obtaining the fibril diameter values, relative frequency distributions were created for each genotype at 370 d and 570 d for comparisons (b). Alterations were consistently present after SLRP knockdown at 300d relative to WT (c), however I-*Dcn*$^{-/-}$/*Bgn*$^{-/-}$ tendons were the only group with no alterations to the collagen fibril distribution compared to WT at 570 d (d). Data shown as median with the box containing quartiles 1–3 and the range spanning the minimum to maximum collagen fibril diameter. Bars indicate significance of $p < 0.05/3$. Kolmogorov-Smirnov tests were used to compare the WT fibril diameter distribution to each experimental group.

gene expression was accompanied by a substantial reduction in decorin and biglycan protein levels in tendon 30 days after Cre induction [11]. Our current study showed similar levels of gene expression after knockdown with a timeline that was 6 to 15 times longer between Cre induction and sacrifice, allowing a greater degree of protein turnover to occur.

This study identified insights into the differential roles of decorin and biglycan during tendon aging without the confounding factor of abnormal tendon development associated with knockout

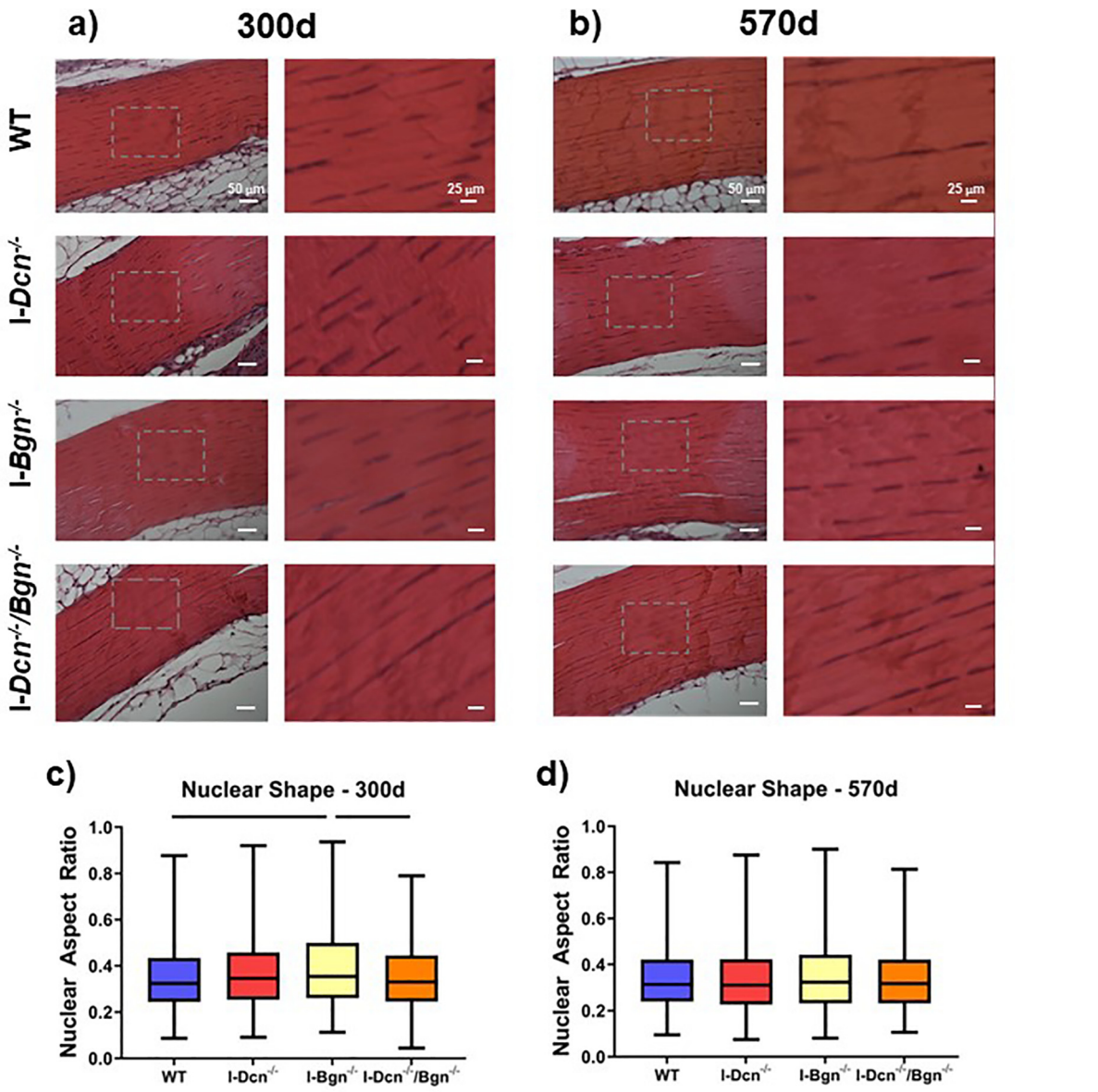

Fig. 6. Patellar Tendon Cellular Nuclear Aspect Ratio After SLRP Knockdown. Tendons were stained with hematoxylin and eosin to visualize the macroscopic collagen structure, cellularity, and nuclear aspect ratio at 300 d (a) and 500 d (b, n = 4/genotype/age). Gray boxes denote areas of higher magnification to show greater detail. No irregularities were noted in the tendon structure, and no changes to cellularity were observed (data not shown). Nuclear aspect ratio was increased in l-*Bgn*$^{-/-}$ tendons at 300 d (c), but no changes were present between genotypes at 570 d (d). Data shown as median with the box containing quartiles 1–3 and the range spanning the minimum to maximum nuclear aspect ratio. Bars indicate significance of $p < 0.05/6$. Kolmogorov-Smirnov tests were used to compare the nuclear aspect ratio distributions between groups.

models. Knockdown of decorin resulted in increased midsubstance modulus and decreased stress relaxation at 300d. However, these changes did not persist at 570d. Knockdown of biglycan resulted in minimal changes to the tendon throughout aging. Interestingly, the compound knockdown of decorin and biglycan resulted in a unique phenotype that was detrimental to overall tendon mechanics and structure.

Experimental procedures

Animal backgrounds & cre excision

This study was approved by the University of Pennsylvania and University of South Florida Institutional Animal Care and Use Committees. Female *Dcn*$^{+/+}$/*Bgn*$^{+/+}$ control (WT, n = 16/age), *Dcn*$^{flox/flox}$ (l-*Dcn*$^{-/-}$, n = 16/age), *Bgn*$^{flox/flox}$ (l-*Bgn*$^{-/-}$, n = 16/age), and compound *Dcn*$^{flox/flox}$/*Bgn*$^{flox/flox}$

(I-*Dcn* $^{-/-}$/*Bgn*$^{-/-}$, n = 16/age), mice with a tamoxifen (TM) inducible Cre, (B6.129-Gt(ROSA)26Sortm1(cre/ERT2)Tyj/J, Jackson Labs) were utilized (Supplemental Fig. 1). Cre excision of the conditional alleles was induced in mature (120 day) mice with three consecutive daily IP injections of tamoxifen (4.5 mg/40 g body weight). WT mice were given TM injections to control for potential side effects. Mice were euthanized at 300 and 570 days of age (n = 16/group/age).

SLRP & collagen I gene expression

Patellar tendons were collected after sacrifice and preserved under liquid nitrogen. The frozen patellar tendons were cut into small pieces, then total RNA was extracted using a RNeasy Micro Kit (Qiagen). Total RNA (4 ng/well) was subjected to reverse transcription using the High-Capacity cDNA Reverse Transcription Kit (Applied Biosystems) and real-time PCR was performed with Fast SYBR Green PCR master mix (Applied Biosystems) using a StepOnePlus Real Time PCR system (Applied Biosystems). The primer sequences were as follows: decorin forward primer, 5′-TGAGCTTCAACAGCATCACC-3′, and decorin reverse primer, 5′-AAGTCATTTTGCC CAACTGC-3′; biglycan forward primer, 5′-CTACG CCCTGGTCTTGGTAA-3′, and biglycan reverse primer, 5′-ACTTTGCGGATACGGTTGTC-3′; fibromodulin forward primer: 5′-GAAGGGTTGTTACG CAAATGG-3′, and fibromodulin reverse primer: 5′-AGATCACCCCCTAGTCTGGGTTA-3′; lumican forward primer, 5′-TCCACTTCCAAAGTCCCTG CAAGA-3′, and lumican reverse primer, 5′-AAGCC GAGACAGCATCCTCTTTGA-3′; keratocan forward primer, 5′- CCTGGAAAGCAAGGTGCTG-TA-3′, and keratocan reverse primer, 5′- TCATAG-GCCTGTCTCACACTCTGT-3′; *Col1a1* forward primer, 5′-CTTCACCTACAGCACCCTTGTG-3′, and *Col1a1* reverse primer, 5′- TGACTGTCTTGC-CCCAAGTTC; β-actin forward primer, 5′- AGATGA-CCCAGATCATGTTTGAGA-3′ and β-actin reverse primer, 5′- CACAGCCTGGATGGCTACGT-3′. The samples were run in duplicate (n = 3–4/group), then the data were analyzed with StepOne software c2.0 (Applied Biosystems). The amount of sample total RNA was standardized by using β-actin as an internal control.

Tendon biomechanics and collagen fiber realignment

Right patellar tendons were prepared for mechanical testing (n = 10–16/genotype/age) as described [6]. Briefly, patella-tendon-tibia complexes were dissected, then scanned using a custom laser device to measure cross-sectional area [38]. Verhoeff's stain was used to apply stain lines at the tibial insertion, 1 mm and 2 mm from the tibial insertion, and at the distal patella for optical strain tracking. The tibia was secured in a custom 3D-printed pot using poly(methyl methacrylate). Custom fixtures were used to secure the pot during mechanical testing.

During testing, tendons were loaded into a 1x phosphate-buffered saline bath at 37 °C secured to a tensile testing system (Instron 5848, Instron, Norwood, MA) integrated with an established cross-polarized light setup [11,39]. The viscoelastic testing protocol consisted of preconditioning, stress relaxations (3 %, 4 %, and 5 % strain) each followed by a series of frequency sweeps (0.1, 1, 5, and 10 Hz), a return to gauge length for 60 s, and ending with a ramp-to-failure at a strain rate of 0.1 %/s. A series of image maps, each consisting of 18 images, was taken throughout the ramp to failure at 20 s intervals for collagen fiber realignment and optical strain tracking data [39]. Collagen fiber realignment, outputted as circular variance ratio, was calculated separately for the tendon midsubstance and insertion using a custom program, and has an inverse relationship with the realignment of collagen fibers (Matlab, Natick, MA) [40]. Circular variance measures the distribution of collagen fiber alignment on the surface of the tendon. The circular variance ratio is the circular variance at a given strain normalized by the circular variance of the same sample at gauge length. Maximum stress was calculated from stress-strain data. Optical tracking was used to compute midsubstance and insertion modulus (Matlab, Natick, MA). Dynamic modulus and phase shift were calculated at each strain-frequency combination.

Collagen fibril diameter

Left patellar tendons were analyzed using TEM (n = 4/genotype/age). Samples were fixed *in situ* using Karnovsky's fixative, then dissected from the mouse and placed in Karnovsky's fixative for an additional 2–4 h [11,41,42]. Post-fixation the samples were rinsed in 0.1 M sodium cacodylate buffer, then placed in a 1 % osmium tetroxide solution for staining and secondary fixation for 1 h. Next, the samples were dehydrated using ethanol solutions (ranging from 50 % to 100 % ethanol in water), then the samples were placed on a shaker for 3 12-hour cycles for epoxy infiltration (ranging from 33 % to 100 % epoxy resin in propylene oxide) and embedded in fresh epoxy resin before being placed in a 60 °C oven overnight for curing. Post-staining with 2 % aqueous uranyl acetate followed by 1 % phosphotungstic acid, pH 3.2 was utilized for contrast enhancement. Cross sections through the midsubstance of the patellar tendons were examined at 80 kV using a JEOL 1400 transmission electron microscope. Images were digitally captured at an instrument magnification of 60,000x using an Orius widefield sidemount CCD camera at a resolution of 3648 × 2672. The digital images were masked and transferred to a RM Biometrics-Bioquant Image Analysis System (Memphis, TN) for analysis. Image magnification was calibrated

using a line grating replica (PELCO®, Product No. 606). Fibril diameter analyses were completed using images from the central portion of the tendon. 10 images were analyzed per animal, and 3500 fibrils were analyzed for each group. All fibrils within a predetermined region of interest (ROI) on the digitized image were analyzed. Non-overlapping ROIs were placed based on fibril orientation (i.e., cross section) and absence of cells. Diameters were measured along the minor axis of the fibril. For measurements of fibril density, the total number of fibrils within the ROI was normalized for area.

Cell nuclear shape and cellularity

For histological analysis, the left knee joint was isolated by cutting through the femur and tibia at the time of sacrifice (n = 4/genotype/age). The knee was flexed to 90°, placed into a cassette, fixed in formalin, and processed using standard paraffin histological techniques. Samples were embedded in paraffin and sections were cut at 7 μm thickness before staining with hematoxylin and eosin. Cell nuclear shape, determined by measuring the nuclear aspect ratio, and cellularity were calculated using commercial software (Bioquant).

Statistics

A two-way ANOVA with Bonferroni post-hoc analysis was used to evaluate the effect of genotype and age on tendon mechanics and cellularity. Realignment data was analyzed using a three-way ANOVA to evaluate the factors of genotype, age, and strain level with Bonferroni post-hoc analysis using the open-source Python package Pingouin [43]. Kolmogorov-Smirnov tests with Bonferroni post-hoc analysis were used in the analysis of collagen fibril diameter and nuclear shape. The significance level was set at $p < 0.05$.

CRediT authorship contribution statement

Zakary M. Beach: Data curation, Formal analysis, Investigation, Methodology, Visualization, Writing – original draft, Writing – review & editing. **Mihir S. Dekhne:** Data curation, Formal analysis, Investigation, Writing – review & editing. **Ashley B. Rodriguez:** Data curation, Software, Writing – review & editing. **Stephanie N. Weiss:** Resources, Writing – review & editing. **Thomas H. Adams:** Data curation, Investigation. **Sheila M. Adams:** Data curation, Investigation. **Mei Sun:** Data curation, Investigation, Writing – original draft. **David E. Birk:** Conceptualization, Funding acquisition, Methodology, Project administration, Supervision, Writing – review & editing. **Louis J. Soslowsky:** Conceptualization, Funding acquisition, Methodology, Project administration, Supervision, Writing – review & editing.

DECLARATION OF COMPETING INTEREST

The authors declare that they have no known competing financial interests or personal relationships that could have appeared to influence the work reported in this paper.

Acknowledgements

This material is based upon work supported by the NSF GRFP (DGE-1845298) and NIH/NIAMS (P30AR069619 and R01AR068057).

Appendix A. Supplementary data

Supplementary data to this article can be found online at https://doi.org/10.1016/j.mbplus.2022.100114.

Received 31 March 2022;
Accepted 14 June 2022;
Available online 24 June 2022

Keywords:
Tendon;
Biomechanics;
Decorin;
Biglycan;
Proteoglycan;
Aging

References

[1]. Zhang, G., Young, B.B., Ezura, Y., Favata, M., Soslowsky, L.J., Chakravarti, S., Birk, D.E., (2005). Development of tendon structure and function: Regulation of collagen fibrillogenesis. *J. Musculoskelet. Neuronal Interact.*, **5**, 5–21. https://doi.org/10.1016/j.biomaterials.2010.02.062.

[2]. Chen, S., Birk, D.E., (2013). The regulatory roles of small leucine-rich proteoglycans in extracellular matrix assembly. *FEBS J.*, **280**, 2120–2137. https://doi.org/10.1111/febs.12136.

[3]. Schonherr, E., Witsch-Prehm, P., Harrach, B., Robenek, H., Rauterberg, J., Kresse, H., (1995). Interaction of biglycan with type I collagen. *J. Biol. Chem.*, **270**, 2776–2783. https://doi.org/10.1074/jbc.270.6.2776.

[4]. Dourte, L.M., Pathmanathan, L., Mienaltowski, M.J., Jawad, A.F., Birk, D.E., Soslowsky, L.J., (2013). Mechanical, compositional, and structural properties of the mouse patellar tendon with changes in biglycan gene expression. *J. Orthop. Res.*, **31**, 1430–1437. https://doi.org/10.1002/jor.22372.

[5]. Dourte, L.M., Pathmanathan, L., Jawad, A.F., Iozzo, R.V., Mienaltowski, M.J., Birk, D.E., Soslowsky, L.J., (2012). Influence of decorin on the mechanical, compositional, and structural properties of the mouse patellar tendon. *J. Biomech. Eng.*, **134**, https://doi.org/10.1115/1.4006200 031005.

[6]. Dunkman, A.A., Buckley, M.R., Mienaltowski, M.J., Adams, S.M., Thomas, S.J., Satchell, L., Kumar, A., Pathmanathan, L., Beason, D.P., Iozzo, R.V., Birk, D.E., Soslowsky, L.J., (2014). The tendon injury response is influenced by decorin and biglycan. *Ann. Biomed. Eng.*, **42**, 619–630. https://doi.org/10.1007/s10439-013-0915-2.

[7]. Dunkman, A.A., Buckley, M.R., Mienaltowski, M.J., Adams, S.M., Thomas, S.J., Satchell, L., Kumar, A., Pathmanathan, L., Beason, D.P., Iozzo, R.V., Birk, D.E., Soslowsky, L.J., (2013). Decorin expression is important for age-related changes in tendon structure and mechanical properties. *Matrix Biol.*, **32**, 3–13. https://doi.org/10.1016/j.matbio.2012.11.005.

[8]. Dunkman, A.A., Buckley, M.R., Mienaltowski, M.J., Adams, S.M., Thomas, S.J., Kumar, A., Beason, D.P., Iozzo, R.V., Birk, D.E., Soslowsky, L.J., (2014). The injury response of aged tendons in the absence of biglycan and decorin. *Matrix Biol.*, **35**, 232–238. https://doi.org/10.1016/j.matbio.2013.10.008.

[9]. J.A. Buckwalter, J. Heckman, An AOA critical issue: aging of the North American population: new challenges for orthopaedics, J. Bone Joint Surg. Am. 85-A (2003) 748–758. http://www.ncbi.nlm.nih.gov/pubmed/12672854 (accessed August 10, 2017).

[10]. Lindemann, I., Coombes, B.K., Tucker, K., Hug, F., Dick, T.J.M., (2020). Age-related differences in gastrocnemii muscles and Achilles tendon mechanical properties in vivo. *J. Biomech.*, **112**, https://doi.org/10.1016/J.JBIOMECH.2020.110067 110067.

[11]. Robinson, K.A., Sun, M., Barnum, C.E., Weiss, S.N., Huegel, J., Shetye, S.S., Lin, L., Saez, D., Adams, S.M., Iozzo, R.V., Soslowsky, L.J., Birk, D.E., (2017). Decorin and biglycan are necessary for maintaining collagen fibril structure, fiber realignment, and mechanical properties of mature tendons. *Matrix Biol.*,. https://doi.org/10.1016/j.matbio.2017.08.004.

[12]. Metzger, D., Clifford, J., Chiba, H., Chambon, P., (1995). Conditional site-specific recombination in mammalian cells using a ligand- dependent chimeric Cre recombinase. *Proc. Natl. Acad. Sci. U. S. A.*, **92**, 6991–6995. https://doi.org/10.1073/pnas.92.15.6991.

[13]. Schwenk, F., Kühn, R., Angrand, P.O., Rajewsky, K., Stewart, A.F., (1998). Temporally and spatially regulated somatic mutagenesis in mice. *Nucleic Acids Res.*, **26**, 1427–1432. https://doi.org/10.1093/nar/26.6.1427.

[14]. Barbieri, R.L., (2009). The Breast. *In: Yen Jaffe's Reprod. Endocrinol.*,. Elsevier, pp. 235–248. 10.1016/B978-1-4160-4907-4.00010-3.

[15]. Best, K.T., Studentsova, V., Ackerman, J.E., Nichols, A.E. C., Myers, M., Cobb, J., Knapp, E., Awad, H.A., Loiselle, A.E., (2021). Effects of tamoxifen on tendon homeostasis and healing: Considerations for the use of tamoxifen-inducible mouse models. *J. Orthop. Res.*, **39**, 1572–1580. https://doi.org/10.1002/jor.24767.

[16]. E. Arias, National Vital Statistics Reports, Volume 61, Number 3, 09/24/2012... for 2008, 61 (2008) 20-21,26-27. https://www.cdc.gov/nchs/data/nvsr/nvsr61/nvsr61_03.pdf.

[17]. Yuan, R., Tsaih, S.-W., Petkova, S.B., de Evsikova, C.M., Xing, S., Marion, M.A., Bogue, M.A., Mills, K.D., Peters, L. L., Bult, C.J., Rosen, C.J., Sundberg, J.P., Harrison, D.E., Churchill, G.A., Paigen, B., (2009). Aging in inbred strains of mice: study design and interim report on median lifespans and circulating IGF1 levels. *Aging Cell.*, **8**, 277. https://doi.org/10.1111/J.1474-9726.2009.00478.X.

[18]. Matthews, C.E., Chen, K.Y., Freedson, P.S., Buchowski, M.S., Beech, B.M., Pate, R.R., Troiano, R.P., (2008). Amount of time spent in sedentary behaviors in the United States, 2003–2004. *Am. J. Epidemiol.*, **167**, 875–881. https://doi.org/10.1093/aje/kwm390.

[19]. Reed, C.C., Iozzo, R.V., (2002). The role of decorin in collagen fibrillogenesis and skin homeostasis. *Glycoconj. J.*, **19**, 249–255. https://doi.org/10.1023/A:1025383913444.

[20]. Robinson, P.S., Huang, T.-F., Kazam, E., Iozzo, R.V., Birk, D.E., Soslowsky, L.J., (2005). Influence of decorin and biglycan on mechanical properties of multiple tendons in knockout mice. *J. Biomech. Eng.*, **127**, 181. https://doi.org/10.1115/1.1835363.

[21]. Fessel, G., Snedeker, J.G., (2009). Evidence against proteoglycan mediated collagen fibril load transmission and dynamic viscoelasticity in tendon. *Matrix Biol.*, **28**, 503–510. https://doi.org/10.1016/j.matbio.2009.08.002.

[22]. Lujan, T.J., Underwood, C.J., Jacobs, N.T., Weiss, J.A., (2009). Contribution of glycosaminoglycans to viscoelastic tensile behavior of human ligament. *J. Appl. Physiol.*, **106**, 423. https://doi.org/10.1152/JAPPLPHYSIOL.90748.2008.

[23]. Corsi, A., Xu, T., Chen, X.D., Boyde, A., Liang, J., Mankani, M., Sommer, B., Iozzo, R.V., Eichstetter, I., Robey, P.G., Bianco, P., Young, M.F., (2002). Phenotypic effects of biglycan deficiency are linked to collagen fibril abnormalities, are synergized by decorin deficiency, and mimic Ehlers-Danlos-like changes in bone and other connective tissues. *J. Bone Miner. Res.*, **17**, 1180–1189. https://doi.org/10.1359/jbmr.2002.17.7.1180.

[24]. Leiphart, R.J., Shetye, S.S., Weiss, S.N., Dyment, N.A., Soslowsky, L.J., (2020). Induced knockdown of decorin, alone and in tandem with biglycan knockdown, directly increases aged murine patellar tendon viscoelastic properties. *J. Biomech. Eng.*, **142** https://doi.org/10.1115/1.4048030.

[25]. A.M. Cribb, J.E. Scott, Tendon response to tensile stress: an ultrastructural investigation of collagen:proteoglycan interactions in stressed tendon., J. Anat. 187 (1995) 423. / pmc/articles/PMC1167437/?report=abstract (accessed May 5, 2022).

[26]. Liao, J., Vesely, I., (2007). Skewness angle of interfibrillar proteoglycans increases with applied load on mitral valve chordae tendineae. *J. Biomech.*, **40**, 390–398. https://doi.org/10.1016/J.JBIOMECH.2005.12.011.

[27]. Lujan, T.J., Underwood, C.J., Henninger, H.B., Thompson, B.M., Weiss, J.A., (2007). Effect of dermatan sulfate glycosaminoglycans on the quasi-static material properties of the human medial collateral ligament. *J. Orthop. Res.*, **25**, 894–903. https://doi.org/10.1002/jor.20351.

[28]. Reese, S.P., Underwood, C.J., Weiss, J.A., (2013). Effects of decorin proteoglycan on fibrillogenesis, ultrastructure, and mechanics of type I collagen gels. *Matrix Biol.*, **32**, 414–423. https://doi.org/10.1016/J.MATBIO.2013.04.004.

[29]. Chen, S., Young, M.F., Chakravarti, S., Birk, D.E., (2014). Interclass small leucine-rich repeat proteoglycan interactions regulate collagen fibrillogenesis and corneal stromal assembly. *Matrix Biol.*, **35**, 103–111. https://doi.org/10.1016/J.MATBIO.2014.01.004.

[30]. Iozzo, R.V., Schaefer, L., (2015). Proteoglycan form and function: A comprehensive nomenclature of proteoglycans. *Matrix Biol.*, **42**, 11–55. https://doi.org/10.1016/j.matbio.2015.02.003.

[31]. Merline, R., Moreth, K., Beckmann, J., Nastase, M.V., Zeng-Brouwers, J., Tralhão, J.G., Lemarchand, P., Pfeilschifter, J., Schaefer, R.M., Iozzo, R.V., Schaefer, L., (2011). Signaling by the matrix proteoglycan decorin controls inflammation and cancer through PDCD4 and microRNA-21. *Sci. Signal.*, **4**, 1–15. https://doi.org/10.1126/scisignal.2001868.

[32]. Melchior-Becker, A., Dai, G., Ding, Z., Schäfer, L., Schrader, J., Young, M.F., Fischer, J.W., (2011). Deficiency of biglycan causes cardiac fibroblasts to differentiate into a myofibroblast phenotype. *J. Biol. Chem.*, **286**, 17365–17375. https://doi.org/10.1074/JBC.M110.192682.

[33]. Berendsen, A.D., Fisher, L.W., Kilts, T.M., Owens, R.T., Robey, P.G., Gutkind, J.S., Young, M.F., (2011). Modulation of canonical Wnt signaling by the extracellular matrix component biglycan. *Proc. Natl. Acad. Sci.*, **108**, 17022–17027. https://doi.org/10.1073/pnas.1110629108.

[34]. Berendsen, A.D., Pinnow, E.L., Maeda, A., Brown, A. C., McCartney-Francis, N., Kram, V., Owens, R.T., Robey, P.G., Holmbeck, K., de Castro, L.F., Kilts, T.M., Young, M.F., (2014). Biglycan modulates angiogenesis and bone formation during fracture healing. *Matrix Biol.*, **35**, 223–231. https://doi.org/10.1016/J.MATBIO.2013.12.004.

[35]. Ezura, Y., Chakravarti, S., Oldberg, A., Chervoneva, I., Birk, D.E., (2000). Differential expression of lumican and fibromodulin regulate collagen fibrillogenesis in developing mouse tendons. *J. Cell Biol.*, **151**, 779. https://doi.org/10.1083/JCB.151.4.779.

[36]. Kalamajski, S., Bihan, D., Bonna, A., Rubin, K., Farndale, R.W., (2016). Fibromodulin interacts with collagen cross-linking sites and activates lysyl oxidase. *J. Biol. Chem.*, **291**, 7951. https://doi.org/10.1074/JBC.M115.693408.

[37]. Kalamajski, S., Liu, C., Tillgren, V., Rubin, K., Oldberg, Å., Rai, J., Weis, M.A., Eyre, D.R., (2014). Increased C-telopeptide cross-linking of tendon type I collagen in fibromodulin-deficient mice. *J. Biol. Chem.*, **289**, 18873. https://doi.org/10.1074/JBC.M114.572941.

[38]. Favata, M., (2006). Scarless Healing in the Fetus: Implications and Strategies for Postnatal Tendon Repair. University of Pennsylvania.

[39]. Lake, S.P., Miller, K.S., Elliott, D.M., Soslowsky, L.J., (2009). Effect of fiber distribution and realignment on the nonlinear and inhomogeneous mechanical properties of human supraspinatus tendon under longitudinal tensile loading. *J. Orthop. Res.*, **27**, 1596–1602. https://doi.org/10.1002/jor.20938.

[40]. Miller, K.S., Connizzo, B.K., Feeney, E., Soslowsky, L.J., (2012). Characterizing local collagen fiber re-alignment and crimp behavior throughout mechanical testing in a mature mouse supraspinatus tendon model. *J. Biomech.*, **45**, 2061–2065. https://doi.org/10.1016/J.JBIOMECH.2012.06.006.

[41]. Birk, D.E., Trelstad, R.L., (1986). Extracellular compartments in tendon morphogenesis: Collagen fibril, bundle, and macroaggregate formation. *J. Cell Biol.*, **103**, 231–240. https://doi.org/10.1083/jcb.103.1.231.

[42]. Birk, D.E., Zycband, E.I., Woodruff, S., Winkelmann, D.A., Trelstad, R.L., (1997). Collagen fibrillogenesis in situ: Fibril segments become long fibrils as the developing tendon matures. *Dev. Dyn.*, **208**, 291–298. https://doi.org/10.1002/(SICI)1097-0177(199703)208:3<291::AID-AJA1>3.0.CO;2-D.

[43]. Vallat, R., (2018). Pingouin: statistics in Python. *J. Open Source Softw.*, **3**, 1026. https://doi.org/10.21105/joss.01026.